

# Magnetism and half-metallicity of some Cr-based alloys and their potential for application in spintronic devices

Yong Liu, College of Science, Yanshan University, Qinhuangdao, Hebei 066004, China  
 S.K. Bose, Physics Department, Brock University, St. Catharines, Ontario L2S 3A1 Canada  
 J. Kudrnovský, Institute of Physics, Czech Academy of Sciences, Prague 8, Czech Republic

## Introduction

Half-metallic (HM) ferromagnetism with relatively high Curie temperatures  $T_c$  (room temperatures and above) is an ideal characteristic of materials with potential for application in spintronic devices. Understandably, then, considerable theoretical and experimental efforts have been devoted in recent years to the search for such materials. Cr-doped dilute magnetic semiconductors (see, e.g., [1]) and some Cr-based alloys (see, e.g., [2]) in zinc blende (ZB) structure have been predicted to exhibit HM ferromagnetism. Akinaga *et al.* [3] have grown ferromagnetic (FM) ZB thin films, which showed  $T_c$  in excess of 400 K. Thin films of CrSb grown by solid-source molecular beam epitaxy on GaAs, (Al,Ga)Sb, and GaSb have been found to be of ZB structure and ferromagnetic with  $T_c$  higher than 400 K[4]. Recently, Deng *et al.* [5] were successful in increasing the thickness of ZB-CrSb films to  $\sim 3$  nm by molecular beam epitaxy using (In,Ga)As buffer layers, and Li *et al.* [6] were able to grow  $\sim 4$  nm thick ZB-CrSb films on NaCl (100) substrates. Sreenivasan *et al.* [7] and Bi *et al.* [8] have reported growing  $\sim 5$  nm thick films of ZB CrTe using molecular beam epitaxy on GaAs (100) substrate via a ZnTe buffer layer. Their measurements of temperature-dependent remanent-magnetization indicate a Curie temperature of  $\sim 100$  K in these films. Our own recent theoretical searches have identified some Cr-based chalcogenides and pnictides [9, 10] as holding promise in this regard. We will discuss some of the highlights of these calculations.

## Method

We have carried out electronic structure calculations using the tight-binding linear muffin-tin orbital (TB-LMTO) [11] and the coherent potential approximation (CPA) [12]. The exchange-correlation potential for this local spin density (LSD) functional method was most often chosen to be the one given by Vosko, Wilk and Nusair [13]. Electronic and magnetic properties of CrX (X=As, Sb, S, Se and Te) and CrAs<sub>50</sub>X<sub>50</sub> (X= Sb, S, Se and Te) were calculated for lattice parameters varying between 5.45 and 6.6 Å, appropriate for some typical II-VI and III-V semiconducting substrates. In our LMTO calculation we optimize the ASA (atomic sphere approximation) errors by including empty spheres in the unit cell.

For several cases, we have checked the accuracy of the LMTO-ASA electronic structures against the full-potential LMTO results [14] and found them to be satisfactory. For the mixed alloys CrAs<sub>50</sub>X<sub>50</sub> (X= Sb, S, Se and Te), the As-sublattice of the ZB CrAs structure is assumed to be randomly occupied by an equal concentration of As and X atoms. The disorder in this sublattice is treated under the coherent potential approximation

(CPA) [12]. For CrTe, calculations were done for three structures: NiAs-type hexagonal (NA), ZB and rock-salt (RS). For these cases we also use the full-potential linear augmented plane-wave (FP-LAPW) method (WIEN2k code[15]).

In order to compute the exchange interactions, we follow the method given by Liechtenstein *et al.* [16]. The total (band) energy is mapped into a Heisenberg spin-Hamiltonian form:

$$H_{\text{eff}} = - \sum_{i,j} J_{ij} \mathbf{e}_i \cdot \mathbf{e}_j, \quad (1)$$

where  $i, j$  are site indices,  $\mathbf{e}_i$  is the unit vector pointing along the direction of the local magnetic moment at site  $i$ , and  $J_{ij}$  is the exchange interaction between the moments at sites  $i$  and  $j$ . Using multiple-scattering formalism, the exchange integral in Eq.(1) can be shown to be given by

$$J_{ij} = \frac{1}{4\pi} \lim_{\epsilon \rightarrow 0^+} \text{Im} \int \text{tr}_L \left[ \Delta_i(z) g_{ij}^\uparrow(z) \Delta_j(z) g_{ji}^\downarrow(z) \right] dz, \quad (2)$$

where  $z = E + i\epsilon$  represents the complex energy variable,  $L = (l, m)$ , and  $\Delta_i(z) = P_i^\uparrow(z) - P_i^\downarrow(z)$ , representing the difference in the potential functions for the up and down spin electrons at site ' $i$ '. In the present work  $g_{ij}^\sigma(z)$  ( $\sigma = \uparrow, \downarrow$ ) represents the matrix elements of the Green's function of the medium for the up and down spin electrons. The quantity  $J_{ij}$  given by Eq. (2) includes direct-, indirect-, double-exchange and superexchange interactions, which are often treated separately in model calculations. The negative sign in Eq.(1) implies that positive and negative values of  $J_{ij}$  are to be interpreted as representing ferromagnetic and antiferromagnetic interactions, respectively. One can obtain the Curie temperature  $T_c$  in mean field approximation (MFA) from

$$k_B T_c^{\text{MFA}} = \frac{2}{3} \sum_{i \neq 0} J_{0i}^{\text{Cr,Cr}}, \quad (3)$$

where the sum extends over all the neighboring shells. An improved description of finite-temperature magnetism is provided by the random phase approximation (RPA), with  $T_c$  given by

$$(k_B T_c^{\text{RPA}})^{-1} = \frac{3}{2N} \sum_{\mathbf{q}} [J^{\text{Cr,Cr}}(\mathbf{0}) - J^{\text{Cr,Cr}}(\mathbf{q})]^{-1}. \quad (4)$$

Here  $N$  denotes the order of the translational group applied and  $J^{\text{Cr,Cr}}(\mathbf{q})$  is the lattice Fourier transform of the real-space exchange integrals  $J_{ij}^{\text{Cr,Cr}}$ . We have calculated the exchange interactions and  $T_c$  for both FM reference state and paramagnetic reference state represented by the disordered local moment (DLM) [17] model. The

FM results follow from the usual spin-polarized calculations, where self-consistency of charge- and spin-density yields a nonzero magnetization per unit cell. Although we call this the FM result, our procedure does not guarantee that the true ground state of the system is ferromagnetic, with the magnetic moments of all the unit cells perfectly aligned. This is because we have not explored non-collinear magnetic states, nor all antiferromagnetic (AFM) states attainable within the collinear model. Indeed, our results for the exchange interactions in some cases do suggest the ground states being of AFM or complex magnetic nature. For lack of a suitable label, we refer to all spin-polarized calculations giving a nonzero local moment as FM state calculations. Within the Stoner model, a nonmagnetic state above the Curie temperature  $T_c$  would be characterized by the vanishing of the local moments in magnitude. An alternate description of the nonmagnetic state is provided by the DLM model, where the local moments remain nonzero in magnitude above  $T_c$ , but disorder in magnitude as well as their direction above  $T_c$  causes the global magnetic moment to vanish. This model can be considered as a disordered binary alloy problem, and treated within the CPA. Estimates of the exchange interactions and  $T_c$  calculated within the DLM model thus portrays the reference state as being paramagnetic. Hence, in effect, estimates of  $T_c$  based on FM and DLM models can be considered as estimates from below and above, respectively, the magnetic transition [10].

## Results

Our density functional calculations show that half-metallicity as well as ferromagnetism survive in most of these Cr-based chalcogenides and pnictides in ZB structure over a wide range of the lattice parameter. Exceptions occur for the chalcogenides, CrS, CrSe, and CrTe, at lower values of the lattice parameters, where large antiferromagnetic interactions compete with weaker ferromagnetic interaction among the Cr-Cr and Cr-chalcogen pairs, suggesting instability of the FM state against antiferromagnetic (AFM) or complex magnetic phases. For the pnictides no antiferromagnetic spin fluctuations are found over a wide range of the lattice parameter, including low values. For details, we refer the readers to our previous publication [10] (see Table II, in particular).

Electron density of states (DOS) in ZB structure Cr-based binary alloys has been discussed in detail by various authors (see, e.g. Ref. [2] and references therein). Here we present results for some mixed ternary alloys, in particular  $\text{CrAs}_{50}\text{Sb}_{50}$  and  $\text{CrAs}_{50}\text{Se}_{50}$ . In Figs.1 and 2 we show the DOS for  $\text{CrAs}_{50}\text{Sb}_{50}$  and  $\text{CrAs}_{50}\text{Se}_{50}$ , for lattice parameters above and below the critical values for the half-metallic character. According to Galanakis and Mavropoulos [2], half-metallicity in ZB CrAs appears between the lattice parameters of 5.45 and 5.65 Å. The latter corresponds to the lattice parameter of the GaAs substrate.

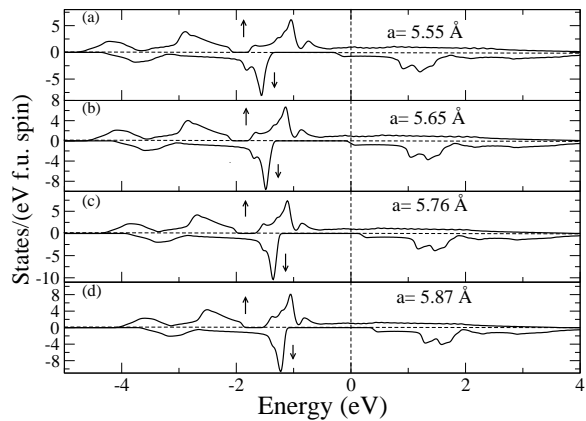


**Figure 1:** Spin-resolved densities of states in ZB  $\text{CrAs}_{50}\text{Sb}_{50}$  for lattice parameters (a) 5.55 Å, (b) 5.65 Å, (c) 5.76 Å and (d) 5.87 Å, respectively.

For CrSb half-metallicity appears at a lattice parameter between 5.65 and 5.87 Å. The mixed alloy  $\text{CrAs}_{50}\text{Sb}_{50}$ , as shown in Fig.1, is not quite half-metallic at the lattice parameter of 5.65 Å, and fully half-metallic at the lattice parameter of 5.76 Å. Replacing Sb with Se in the above alloy, i.e. for  $\text{CrAs}_{50}\text{Se}_{50}$ , brings the critical lattice parameter down slightly. As shown in Fig.2, at a lattice parameter of 5.65 Å,  $\text{CrAs}_{50}\text{Se}_{50}$  is half-metallic, although barely so. In our calculation CrS and CrSe are half-metallic at a lattice parameter of 5.65 Å, and not so at a lattice parameter of 5.55 Å. CrTe is not half-metallic at a lattice parameter of 5.76 Å, but at a lattice parameter of 5.87 Å. For both CrS and CrSe the critical value should be close to 5.65 Å, and for CrTe it should be close to 5.87 Å.

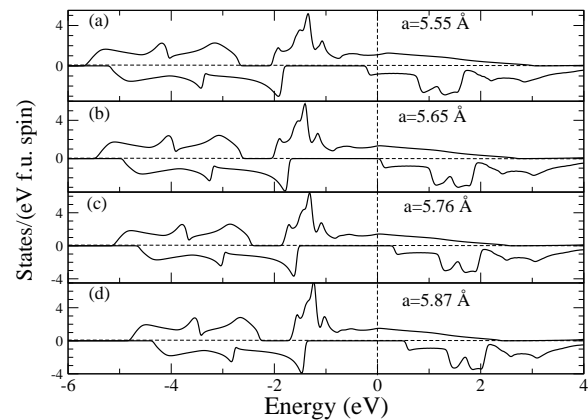


**Figure 2:** Spin-resolved densities of states in ZB  $\text{CrAs}_{50}\text{Se}_{50}$  for lattice parameters (a) 5.55 Å, (b) 5.65 Å, (c) 5.76 Å and (d) 5.87 Å, respectively.

Note that in general the half-metallic gap is larger in the chalcogenides than in the pnictides. This is due to

larger Cr-moment for the chalcogenides, which results in larger exchange splitting. This explains the difference in the half-metallic gaps in Figs. 1 and 2 for similar lattice parameters.

Fig.3 shows the variation of the magnetic moment with the lattice parameter for the random alloys  $\text{CrAs}_{50}\text{X}_{50}$  ( $\text{X}=\text{Sb}, \text{S}, \text{Se}, \text{Te}$ ), where 50% of the As-sublattice is randomly occupied by X-atoms. The saturation moment per f.u. for  $\text{CrAs}_{50}\text{Sb}_{50}$  in the half-metallic state is  $3\mu_B$ , with the results falling between those for CrAs and CrSb. For  $\text{CrAs}_{50}\text{X}_{50}$  ( $\text{X}=\text{S}, \text{Se}, \text{Te}$ ), the saturation moment per f.u. is  $3.5\mu_B$ . The local Cr-moment deviates from the saturation value in the half-metallic state, being higher than the saturation value for all lattice parameters above  $6.1\text{\AA}$ . Our spin-polarized calculations for the FM reference states lead to local moments not only on the Cr atoms, but also on the other atoms (As, Sb, S, Se, and Te) as well as the empty spheres. The DLM state results are free from such induced moments. The moment per f.u. reaches the saturation values of  $4\mu_B$  for the pnictides and  $3\mu_B$  for the chalcogenides in the half-metallic state.

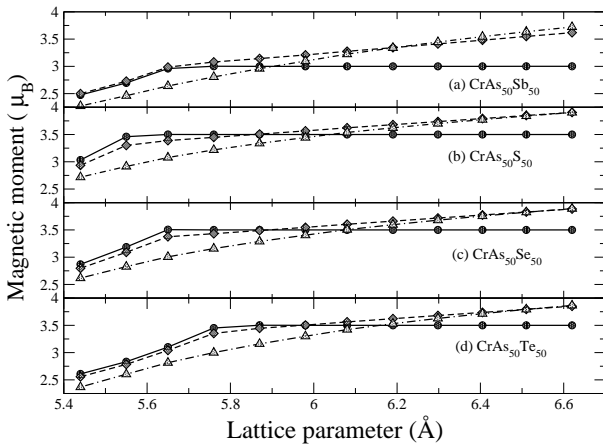


**Figure 3:** A comparison of the moment/f.u. with the local Cr moment in the FM state as well as the DLM state for ZB (a)  $\text{CrAs}_{50}\text{Sb}_{50}$ , (b)  $\text{CrAs}_{50}\text{S}_{50}$ , (c)  $\text{CrAs}_{50}\text{Se}_{50}$ , and (d)  $\text{CrAs}_{50}\text{Te}_{50}$ . Circle: moment/f.u.- FM state, diamond: local Cr-moment- FM state, triangle: local Cr-moment- DLM state.

The saturation values of the moments for all these alloys satisfy the so-called "rule of 8":  $M = (Z_{\text{tot}} - 8)\mu_B$ , where  $Z_{\text{tot}}$  is the total number of valence electrons in the unit cell [2]. The number 8 accounts for the fact that in the half-metallic state the bonding  $p$  bands are full, accommodating 6 electrons, and so is the low-lying band formed of the  $s$  electrons from the  $sp$  atom, accommodating 2 electrons. The magnetic moment then comes from the remaining electrons filling the  $d$  states, first the  $e_g$  states and then the  $t_{2g}$ . The saturation value of  $3\mu_B/\text{f.u.}$ , or the half-metallic state, appears for a larger critical lattice constant in CrSb than in CrAs. Similarly, the critical lattice constants for the saturation magnetic moment of  $4\mu_B/\text{f.u.}$  are in increasing order for CrS, CrSe and CrTe.

$T_c$  for CrAs and CrSb ZB alloys and for lat-

tice parameters appropriate to group II-VI and III-V semiconductor substrates, calculated for FM and DLM reference states are shown in Fig.4.

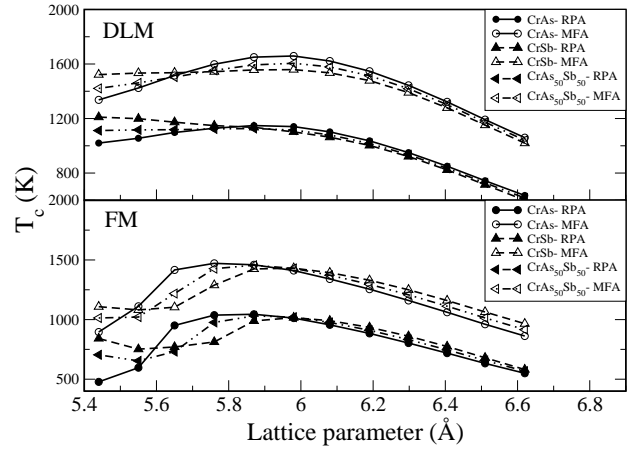
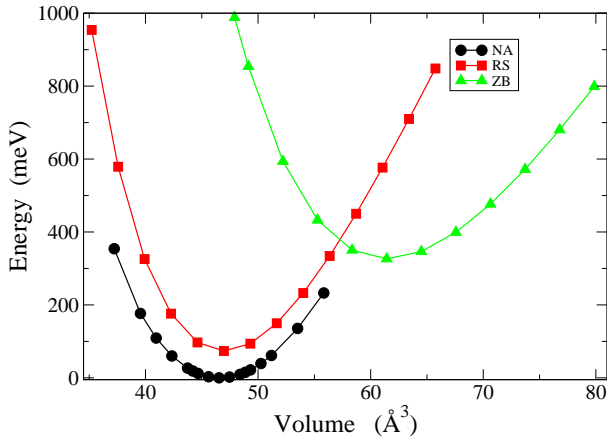


**Figure 4:** Curie temperatures in ZB CrAs and CrSb compounds for FM and DLM reference states. For comparison, the results for the mixed alloy  $\text{CrAs}_{50}\text{Sb}_{50}$  are also shown.

Because of uncertainties related to the induced (non-robust) moments on the non-Cr atoms, including empty spheres, for the FM reference states, estimates of  $T_c$  for the DLM states should be considered more reliable [10]. The indicated values clearly point to the possibility of high temperature half-metallic ferromagnetism in these Cr-based pnictides.

Our results are mostly for the zinc blende (ZB) structure. However, for CrTe we have carried out additional calculations. Bulk samples of CrTe are known to crystallize in NiAs-type (NA) hexagonal structure [18] with cell parameters  $a = 3.997\text{\AA}$ ,  $c = 6.222\text{\AA}$  at room temperature. Both RS and ZB structures are interesting from the standpoint of growing CrTe-films on semiconductor substrates. It is useful to compare the RS and the ZB structure results, because of the different levels of hybridization (even for the same lattice parameter) between the Cr-3d orbital and the  $sp$  orbitals of chalcogen/pnictogen atom. We carried out a systematic structural optimization of NA, ZB, and RS CrTe in FM, NM (non-spin polarized) and AFM configurations. For the NA structure, the  $c/a$  ratio was optimized and the result  $c/a = 1.542$  for the FM phase is in good agreement with previously obtained result [19]. This optimized  $c/a$  ratio was used for the final NA structure volume optimization. We find the RS phase to be more stable than the ZB phase. Hence we have considered three structures: ZB, RS and NA. Results of energy optimization for these three structures, using the FP-LAPW code (WIEN2k) and the generalized gradient approximation (GGA) [20], are shown in Fig.5. The ZB and RS phases are higher in energies than NA by 0.328 eV and 0.076 eV/atom, respectively. However, the RS structure is only marginally unstable against the NA structure, and more stable than the ZB structure, with an energy that is about 0.25 eV/atom lower. According to our calculation, the ZB phase is more stable than the RS

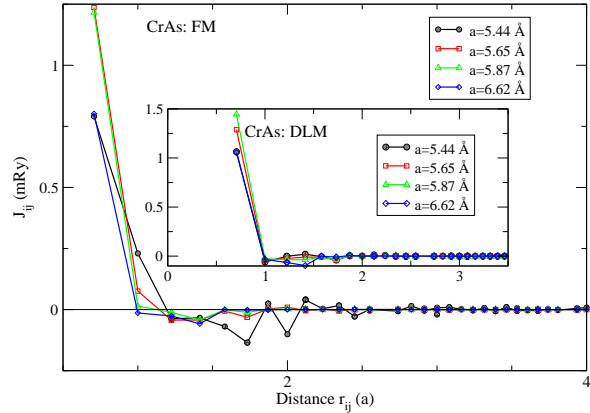
phase for volumes per atom greater than  $57 \text{ \AA}^3$  (Fig. 5).



**Figure 5:** (Color online) Energy as a function of volume per atom in the three structural phases of CrTe, obtained via FP-LAPW GGA (WIEN2k) method.

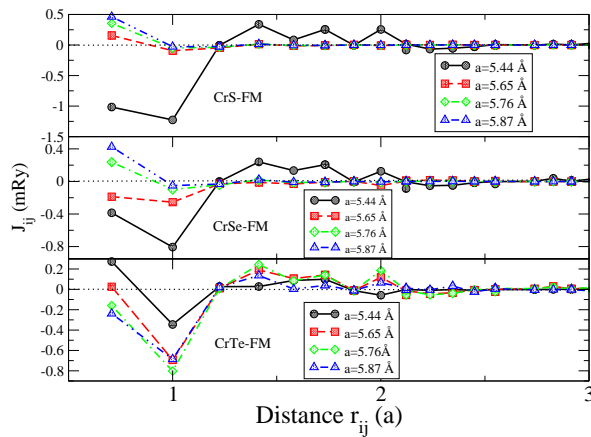
It should be possible to stabilize the RS phase at lower volumes. Recently, Sreenivasan *et al.* [7] and Bi *et al.* [8] were able to grow ZB CrTe films on GaAs substrates. Their measured values of the lattice parameter lie in the range 6.1-6.21  $\text{\AA}$ , corresponding to volumes per atom 57-59.9  $\text{\AA}^3$ . Our calculations suggest that in order to grow RS CrTe one should consider suitable substrates with lattice parameters less than 6.1 or 6.0  $\text{\AA}$ . For further details, readers should consult our recent publication [9].

structure for the chalcogenides CrS, CrSe and CrTe at low values of the lattice parameter, is shown in Fig.6. It should be noted that for the pnictrides CrAs and CrSb the AFM interactions are much more suppressed.



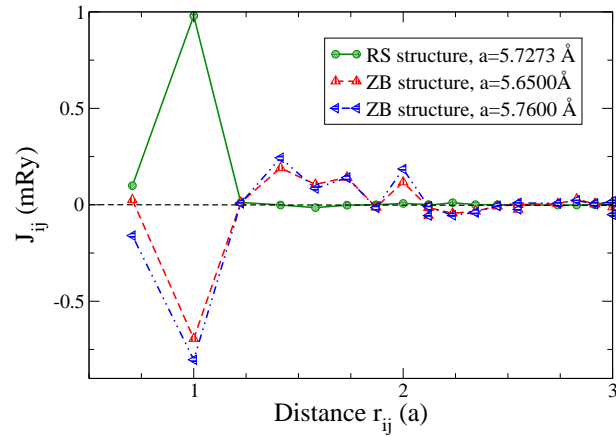
**Figure 7:** (Color online) Distance dependence of the exchange interaction between the Cr atoms in CrAs for various lattice parameters  $a$ , calculated for the FM and DLM reference states.

Fig.7 shows the Cr-Cr exchange interactions in CrAs for both FM and DLM reference states for a wide range of the lattice parameter. Fig.8 shows that for CrTe in the RS structure the Cr-Cr interactions are entirely ferromagnetic, whereas for similar lattice parameters or volumes/atom these have a significant AFM component for the ZB phase.



**Figure 6:** (Color online) Distance-dependence of the Cr-Cr exchange interaction for the ZB structure Cr-chalcogenides for the FM reference state. The distance between the Cr atoms in Figs. 6-8 is given in units of the lattice parameter  $a$ .

The RS phase is interesting, as it is found to be free from AFM spin fluctuations, which are prevalent in the ZB phase, particularly at low values of the lattice parameter. As a result, the  $T_c$  for RS CrTe is higher than that of the ZB phase for all lattice parameters. Preponderance of AFM interactions in the ZB



**Figure 8:** (Color online) Exchange interaction, computed by using the LMTO-Green's function method, between the Cr atoms in the ZB and RS structures CrTe as a function of the lattice parameter. The two lattice parameters for the ZB structure chosen are above and below the equilibrium lattice parameter 5.727  $\text{\AA}$  for the RS structure, obtained in the FP-LAPW GGA (WIEN2k) calculation.

In Fig.9 we compare the  $T_c^{RPA}$  values for RS and ZB CrTe, obtained by using the TB-LMTO-Green's function method and using only the exchange interactions between the Cr atoms (strong moments). The reference

state used for the calculation is the FM state. For the ZB phase, the use of Eq.(4) of Ref. [10] neglecting all the induced moments results in unphysical negative  $T_c$  in the lattice parameter range  $\sim 5.7$ - $6.0$  Å because of dominant AFM Cr-Cr exchange at the nearest and next nearest neighbor sites. Since the exchange calculations are done with respect to a 'FM' reference state with parallel magnetic moments, negative values of the exchange interactions, and in particular the exchange constant  $J_0 = \sum_j J_{0j}$ , imply instability of the reference 'FM' state.

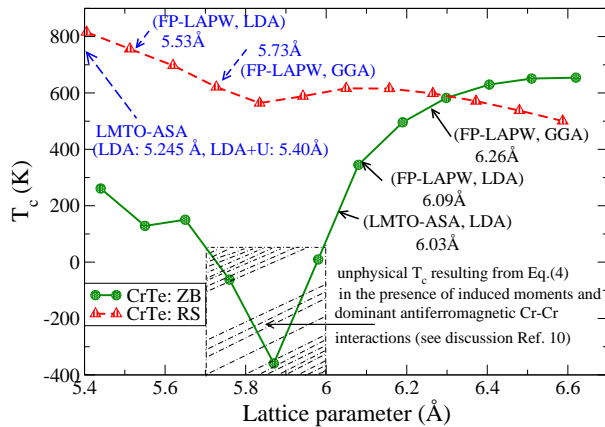


**Figure 9:** (Color online) The RPA Curie temperature as a function of the lattice parameter for the ZB and RS structures of CrTe, calculated by considering the Cr-Cr interaction only and by using the FM reference state. The arrows indicate the equilibrium lattice parameter values according to various calculations. The results for  $T_c$  are somewhat affected by the 'induced' moments on the Te atoms as well as the empty spheres used in the LMTO Green's function calculation. For ZB CrTe, this error, combined with strong AFM spin fluctuation for the lattice parameters in the range  $\sim 5.7$ - $6.0$  Å, results in unphysical negative values of  $T_c$  in this range (see text and also the discussion in Ref. [10] for details). Away from this range  $T_c$  values are reliable, although somewhat underestimated.

The ZB phase has been discussed in detail in our previous publication[10], where we showed that in spite of these nearest and next nearest neighbor AFM interactions, the FM state is lower in energy than the AFM[001] and AFM[111] states. The cumulative effect of the interactions involving the more distant pairs of Cr atoms, and particularly those due to the induced moments, may stabilize the FM phase. Alternatively, the magnetic state is possibly complex, different from FM, AFM[001] and AFM[111]. If the magnetic state is indeed FM, then according to the prescription of Sandratskii *et al.* [21]  $T_c$  should be enhanced with respect to the value given by Eq.(4) and may be positive but small. Note that Sreenivasan *et al.* [7] and Bi *et al.* [8] report the lattice parameters for their ZB CrTe thin films grown on GaAs substrates to be in the range 6.1-6.21 Å and their measurements of remanent magnetization indicate  $T_c \sim 100$  K. This is not too far off from the calculated values 200-400 K shown in Fig. 9. For RS CrTe, on the other hand, all dominant interactions are FM, and as a result the  $T_c$

calculated by using Eq.(4) of Ref. [10] and based on only Cr-Cr interactions give positive values. The actual  $T_c$ s are most probably higher than what is shown in Fig.9.

Magnetism is strongly dependent on the correlation effects. Even though correlation in metallic states is usually well-described within the local density approximation (LDA), different treatments of the exchange and correlation potential may lead to different magnetic moments. The effect of enhanced correlation can be incorporated via the LDA+U method [22]. We find that for CrTe the use of the LDA+U method, with  $U=0.075$  Ry and  $J=0$ , brings the magnetic moment values in close agreement with those given by GGA in the FP-LAPW method (WIEN2k code). In Fig.10, we compare the  $T_c$  values calculated for RS CrTe for the FM reference state, using LDA and LDA+U (with  $U=0.075$  Ry), and for the DLM reference state using LDA. The results shown use the RPA and up to 111 shells of neighbors to insure convergence of the calculated values. Within the uncertainties of our results there seems to be no appreciable difference between the predictions of LDA and LDA+U.

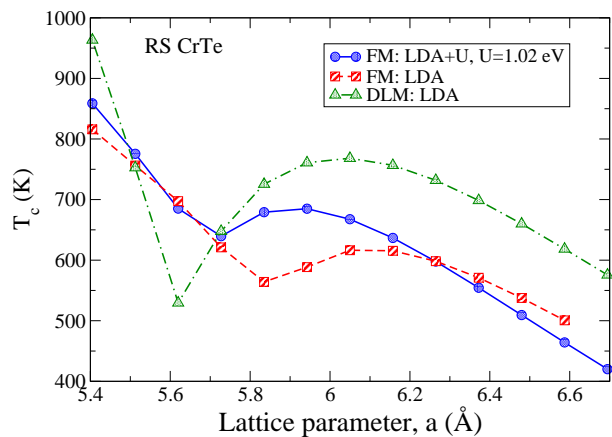


**Figure 10:** (Color online) Comparison of the Curie temperature in RS CrTe calculated for the FM reference states in RPA using the LMTO-ASA scheme and LDA and LDA+U methods.

In Fig.11 we show the  $T_c$  values for the mixed pnictide-chalcogenide alloys  $\text{CrAs}_{50}\text{X}_{50}$  ( $X=\text{S}, \text{Se}$  and  $\text{Te}$ ). Because of significant antiferromagnetic interactions in the chalcogenides for low values of the lattice parameter the FM reference is not ideal for the calculation of  $T_c$  in these cases. The preponderance of AFM interactions suggests that the ground state might not be FM for low lattice parameter values. In such cases the DLM state might be closer to the ground state than the FM state. In addition, the presence of induced moments for the FM configuration necessitates the use of multi-sublattice MFA/RPA calculations. In view of that we present results only for the DLM model. The mixed alloy cases are interesting to study inasmuch as they provide some flexibility in the manipulation of the lattice parameter via concentration variation. Note that the RPA values are lower as well as more reliable estimates of  $T_c$  than those given by MFA, which is known to significantly overestimate the Curie temperature.

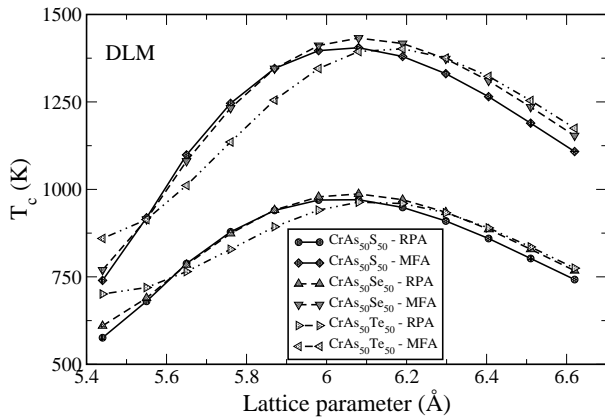


**Figure 11:** Variation of Curie temperature as a function of lattice parameters in ZB  $\text{CrAs}_{50}\text{X}_{50}$  alloys with  $X=\text{Sb}, \text{S}, \text{Se}$  and  $\text{Te}$ . As can be expected, the results for the Curie temperature in ZB  $\text{CrAs}_{50}\text{Sb}_{50}$  fall, in between those of  $\text{CrAs}$  and  $\text{CrSb}$ , as shown in Fig.7. All results shown are for DLM reference states, and as such, should be considered as upper limits for  $T_c$ .

## Conclusions

Our *ab initio* studies of the electronic structure, magnetic moments, exchange interactions and Curie temperatures in ZB  $\text{CrX}$  ( $X=\text{As}, \text{Sb}, \text{S}, \text{Se}$  and  $\text{Te}$ ) and  $\text{CrAs}_{50}\text{X}_{50}$  ( $X=\text{Sb}, \text{S}, \text{Se}$  and  $\text{Te}$ ) reveal that half-metallicity in these alloys is maintained over a wide range of lattice parameters. The results for the exchange interaction and the Curie temperature show that these alloys have relatively high Curie temperatures, i.e. room temperature and above. The exceptions occur for the alloys involving  $\text{S}, \text{Se}$  and  $\text{Te}$  at some low values of lattice parameters, where significant inter-atomic antiferromagnetic exchange interactions indicate ground states to be either antiferromagnetic or of a complex magnetic nature. Our results for the Curie temperature, the lattice Fourier transform of the exchange interactions, and the resulting stability analysis are based on the exchange interactions between the  $\text{Cr}$  atoms only. Because our method yields induced magnetic moments on the non- $\text{Cr}$  atoms, including some of the empty spheres, the results for  $T_c$  and the lattice Fourier transforms contain some errors. However, since the  $\text{Cr}$ -moments and the  $\text{Cr}$ - $\text{Cr}$  exchange interactions are by far the strongest ones, the errors should be small enough to provide qualitative insights to experimentalists in the field. For the purpose of the lattice matching with a given substrate, one can resort to alloying on the non- $\text{Cr}$  sublattice, combining pnictogens with chalcogen atoms. As long as the concentration of the pnictogens is higher than that of the chalcogens, the FM state in the ZB structure should be a stable half-metal with a relatively large value of  $T_c$ .

For the chalcogenide  $\text{CrTe}$  we have explored the relative stability of ZB and RS structures. Although the ground state of this compound is  $\text{NiAs}$ -type hexagonal, at high values of volume/atom the ZB structure has

lower energy. In addition, for some range of the lattice parameter (Fig.5) the RS structure is more stable than ZB. In the RS phase  $\text{CrTe}$  is free from AFM interactions. According to our results, the chalcogenide  $\text{CrTe}$  should be stable in the RS phase at lattice parameters less than  $6.1 \text{ \AA}$ , and should exhibit HM- FM behavior with relatively high  $T_c$ .

Future work in this regard, some of which is already in progress, should involve a systematic comparative study of stability, ferromagnetism and half-metallicity in all of the  $\text{Cr}$ -based chalcogenides and pnictides.

## ACKNOWLEDGMENTS

This work was supported by a grant from the Natural Sciences and Engineering Research Council of Canada. J.K. acknowledges financial support from AV0Z 10100520 and the Czech Science Foundation (202/09/0775).

## References

1. H. Saito, V. Zayets, S. Yamagata, and K. Ando, *Phys. Rev. Lett.* **90**, (2003) 207202.
2. I. Galanakis and P. Mavropoulos, *Phys. Rev.* **B67** (2003) 104417.
3. H. Akinaga, T. Manago, and M. Shirai, *Jpn. J. Appl. Phys.* **40** (2001) L651.
4. J.H. Zhao, F. Matsukura, K. Takamura, E. Abe, D. Chiba, and H. Ohno, *Appl. Phys. Lett.* **79** (2001) 2776.
5. J.J. Deng, J.H. Zhao, J.F. Bi, Z.C. Niu, F.H. Yang, X.G. Wu, and H.Z. Zheng, *J. Appl. Phys.* **99** (2006) 093902.
6. S. Li, J-G Duh, F. Bao, K-X Liu, C-L Kuo, X. Wu, Liya Lü, Z. Huang, and Y Du, *J. Phys. D: Appl. Phys.* **41** (2008) 175004.
7. M.G. Sreenivasan, J.F. Bi, K.L. Teo, and T. Liew, *J. Appl. Phys.* **103** (2008) 043908.
8. J.F. Bi, M.G. Sreenivasan, K.L. Teo, and T. Liew, *J. Phys. D: Appl. Phys.* **41** (2008) 045002.
9. Y. Liu, S.K. Bose, and J. Kudrnovský, *Phys. Rev.* **B82**, (2010) 094435 ; see also references therein.
10. S.K. Bose, J. Kudrnovský, *Phys. Rev.* **B81**, (2010) 054446 ; see also references therein.
11. O.K. Andersen and O. Jepsen, *Phys. Rev. Lett.* **53** (1984) 2571; see also <http://www.fkf.mpg.de/andersen/>.
12. J. Kudrnovský and V. Drchal, *Phys. Rev.* **B41**,(1990) 7515 .
13. S.H. Vosko, L. Wilk, and M. Nusair, *Can. J. Phys.* **58**, (1980) 1200 .
14. S.Yu. Savrasov, and D.Yu. Savrasov, *Phys. Rev.* **B46**, (1992) 12181 .
15. P. Blaha, K. Schwarz, G. K. H. Madsen, D. Kvasnicka and J. Luitz, *WIEN2k, An Augmented-Plane-Wave+ local Orbitals program for Calculating Crystal Properties*, (Karlheinz Schwarz, Tech. Wien, Austria) ISBN 3-9501031-1-2, 2001.

16. A.I. Liechtenstein, M.I. Katsnelson and V.A. Gubanov, *J. Phys.F: Met.Phys.* **14**, (1984) L125.
17. V. Heine, *Solid State Physics* **35** (Academic Press, New York), (1980) 1.
18. M. Chevreton, E.F. Bertaut, and F. Jellinek, *Acta Crystallogr.* **16** (1963) 431.
19. F. Ahmadian, M.R. Abolhassani, S.J. Hashemifar, and M. Elahi, *J. Magn. Magn. Mater.* **322** (2010) 1004.
20. J. P. Perdew, K. Burke and M. Ernzerhof, *Phys. Rev. Lett.* **77** (1996) 3865.
21. L.M. Sandratskii, R. Singer, and E. Sasioglu, *Phys. Rev. B* **76** (2007) 184406.
22. see e.g., V.I. Anisimov, F. Aryasetiawan, and A.I. Liechtenstein, *J. Phys.: Condens. Matter* **9** (1997) 767.